Scaling of Small-Angle Neutron Scattering Intensities from Gelling Colloidal Silica[1]

B.D. Butler,[2,3] C.D. Muzny,[2] and H.J.M. Hanley[2]

---

1. Paper Presented at the Thirteenth Symposium on Thermophysical Properties, June 22-27, 1997, Boulder Colorado, U.S.A. Contribution of the National Institute of Standards and Technology, not subject to copyright in the U.S.

2. Physical and Chemical Properties Division, National Institute of Standards and Technology, Boulder, Colorado 80303, U.S.A.

3. To whom correspondence should be addressed.

ABSTRACT

Small-angle neutron scattering data, taken as a function of time from initiation of gelation in colloidal silica suspensions with silica mass fractions ranging from 15% to 30%, are presented. Over a wide range of initial pH, the measured structure factor $S(q)$ contains a low angle peak that, as time progresses, grows in height and moves to lower wavevectors q. Sometime after the gels have set, this peak stops growing, marking the end of the reaction. The data scale according to the relation $S(q,t) \sim q_m^{-d_f}(t)\tilde{S}(q/q_m(t))$, where $q_m(t)$ is the wavevector location of the low angle peak as a function of time t from initiation, d_f is a fractal dimension, and $\tilde{S}$ is a characteristic structure function. The exponent d_f is insensitive to the silica mass fraction but that the form of $\tilde{S}$ is mass fraction dependent.

KEY WORDS: gels, small-angle scattering, scaling, fractal, colloidal silica,

1. INTRODUCTION

Scattering experiments using light, x-rays, and neutrons, have shown that many silica (and other) gels obey the relation $S(q) \sim q^{-d_f}$ where $S(q)$ is the measured structure factor and q is the wavevector of the scattered radiation [1-3]. Because this power-law behavior is consistent with the scattering predicted from a fractal object, the exponent d_f is normally referred to as the gel's fractal dimension. According to the fractal model, the power law will be observed only over a range of wavevectors which probe length scales larger than the fundamental unit of the gel (a particle of size 7–24 nm for gels made from colloidal silica, for example) but smaller than the average size of the fractal aggregates produced during gelation [4] which ultimately coalesce to form the gel. Strictly, the power-law is also correct only when correlations between aggregates are absent, as in a dilute noninteracting solution. In the presence of interactions the structure factor will deviate from the power-law, perhaps giving rise to a peak in the structure factor at a wavevector related to the dominant correlation length in the system.

In a relatively dilute solution ($\sim 0.03\%$ by volume) of aggregating polystyrene spheres, Carpineti and Giglio [5] found such a correlation peak at small wavevectors and discovered that the structure factor at various times during the aggregation process followed the relation $S(q,t) \sim q_m^{-d_f}(t)\tilde{S}(q/q_m(t))$. Here, $q_m(t)$ is the wavevector location of the low angle peak as a function of time, and $\tilde{S}$ is a characteristic structure function. At larger wavevectors (far from the peak location), the power-law relation also held, and the value of d_f derived from the power-law and scaling analyses were the same. Computer simulation of the decomposition of a Lennard-Jones system at reduced density near 30% [6,7] and measurements of the structure factor in a gel made of colloidal silica with a mass fraction of 30% [8] have also recently been shown to scale by the above relation. In these later two examples, however, the density was high and correlations were strong, so there was no regime in which the power-law relation could be trusted to yield a meaningful exponent. Scaling of the structure factor with time during aggregation is thus a powerful - perhaps indispensable - tool for obtaining exponents for dense aggregating systems.

In this paper we report on measurements of the small angle neutron scattering from gels made of 7 nm diameter colloidal silica particles. Mass fractions ranging from 15% to 30% were investigated and a range of initial pH changes – used to initiate the gelation reaction – were also studied. Scaling of the data was attempted as both a function of time since initiation and as a function of pH.

2. EXPERIMENTAL

Small-angle neutron scattering intensities from the gels were measured on the NG3 spectrometer at the NIST Cold Neutron Research Facility (CNRF). The neutron wavelength was set at $\lambda = 0.5$ nm, and the sample-to-detector distance was 13.15 m. In this configuration, the measurable wavevector range is 0.03 $nm^{-1} < q < 0.42$ nm^{-1}, where $q = 4\pi \sin(\theta/2)/\lambda$ and θ is the scattering angle. Intensities were collected by an area detector and corrected for sample cell and background contributions and variations in detector efficiency. The corrected data were circularly averaged and then normalized to absolute units by comparing the measured count rate to that from a (flat) H_2O standard.

Gels with mass fractions of 30%, 25%, 20%, and 15% were studied. The samples were prepared by adding the appropriate amount of deionized H_2O to stock Ludox SM–30 [9], which is a 30% by mass suspension of 7 nm diameter colloidal silica particles stabilized in an aqueous medium of pH = 10. Gelation of a given sample was initiated by adding concentrated HCl to the suspension thus lowering its pH. Samples with a range of pH from about 4 to 8 were created for each of the four sample densities. Immediately following gel initiation, the solutions were transferred to 1 mm gap-width quartz cells for measurement in the neutron spectrometer. The 30% and 15% by mass samples were studied as a function of time from gel initiation by measuring the structure factor approximately 5 min after addition of the HCl and then every half hour until the gelation reaction was complete. The duration of each of these measurements was 5 min. Measurements of the structure factor from the 25% and 20% by mass samples were made as a function of pH on samples long after (~2 days) the gels had been created and were not followed as a function of

time.

3. RESULTS

Figure 1 shows the diffraction data normalized to absolute scattering units as a function of time from gel initiation for 30% (Fig. 1a) and 15% (Fig. 1b) by mass samples prepared with a pH near the middle of the range studied. A peak in the structure factor at low angles is clearly present in the 30% sample. This peak is observed to grow in height with time while shifting to slightly smaller angles. The growth of this peak is relatively rapid during the first 3 h and then slows down markedly as the gel sets. Only minor changes in the measured scattering occur after about 10 h indicating that at this time the gelation reaction is essentially complete. By contrast, a peak is not observed in the 15% data. A rise in scattering with decreasing angle is observed, however, and like the 30% by mass sample the magnitude of this small-angle scattering increases with time. The evolution of this sample was followed for 8.5 h — enough time to observe significant slowing of the rate of change of the small angle scattering, but not enough time to follow gelation reaction to completion [10].

The fact that no peak was observed in the 15% sample does not necessarily mean that the origins of the rise in scattering are different between the data displayed in Figs. 1a and 1b. More likely, there is a peak, but the low-q limits of the neutron spectrometer prevent us from observing it. This possibility is supported when the data from the 25% and 20% samples are compared to those from the 30% and 15% samples. Figure 2 shows measured structure factors, as a function of pH, for each of these four densities. The data in these plots are from gels prepared approximately 48 h before measurement. As in Fig. 1a there is a clear peak in the 30% samples (Fig. 2a). A peak is also observed in the 25% samples (Fig. 2b) but is obviously closer to the limits of the spectrometer. The data from the 20% samples (Fig. 2c) at a pH of 7.20 and 6.04 also indicate a peak but it appears that any such peak in the sample with a pH of 4.63 is beyond the limits of the spectrometer. Finally, for the 15% samples (Fig. 2d), as in Fig.1a, peaks at lower angles are not apparent. We thus conclude

that in all of the samples measured that there is a peak in the structure factor at small angles – whether observable on this instrument or not – and that its height increases and moves towards lower wavevectors as a function of time after initiation, or as a function of decreasing pH.

4. DISCUSSION

Peaks in the structure functions indicate that there are correlations in these systems. Since there is no simple way to determine the degree of correlation between the aggregates (because the small-angle scattering could be dominated by the internal structure of the aggregates, correlations between the aggregates, or more likely, a combination of both [11]), it is not appropriate to use a power-law slope from the measured scattering to characterize these gels. The scaling relation $S(q,t) \sim q_m^{-d_f}(t)\tilde{S}(q/q_m(t))$ discussed in the introduction, however, does not demand that correlations be absent in the system – in fact, correlations may make it easier to scale the data. All that the scaling relation requires is that the structure factor at various times have the same form $\tilde{S}(X)$ and that the scattering density increases with some characteristic length scale of the system (q_m^{-1}, for example) raised to the power d_f. Depending on the material, d_f can be either the Euclidean dimension [12] or a mass fractal dimension [5].

For the 30% by mass data of Fig. 1a, it is simple to see how the scaling relation is used. First, the location of the correlation peak q_m is determined for each of the curves, the wavevector is scaled by q_m, the structure factor magnitude is modified by $q_m^{-d_f}$, and then the scaled data sets are plotted together. The exponent d_f, however, needs to be determined. Here, we constructed scaling plots for a range of exponents and found that exponent which provided the best fit. For the 30% sample of Fig. 1a the data fall on a single curve for only a relatively narrow range of values centered around $d_f = 1.44 \pm 0.1$ – an outcome consistent with analysis of similar data reported recently [8]. The result is presented in Fig. 3a.

It is not at first clear how such an analysis could be performed for the 15% data since the correlation peaks are beyond the limits of measurement and thus cannot be used to define

the set of q_m. The values of q_m, however, do not need to come from the correlation peak position. For the scaling relation to hold any consistent measure of a characteristic scale can be used – the location of an inflection point in the measured structure factor for instance [13]. Unfortunately, we were unable to define such a consistent measure for these data. Instead we solved not only for the best value of the exponent d_f but also for the best values to assign to the set of q_m (but keeping one of the q_m fixed). It may seem by allowing the q_m to vary this way, that scaling could be achieved for nearly any choice of d_f, or worse, any choice of data sets. Luckily, the solutions to this scaling problem are not that flexible, because the choice of q_m fixes the scale of both the horizontal and vertical axes since d_f is kept constant over all data sets. The data could not be scaled to fit on a universal curve unless the exponent was chosen in the range $d_f = 1.41 \pm 0.1$. Other choices for d_f, regardless of the set of q_m tried, failed to place the measurements on a single curve. The result of this analysis is shown in Fig. 3b.

Interestingly, the exponent for both the 30% and 15% samples are within experimental uncertainty of each other. This may lead one to speculate that the structure of the 30% and the 15% samples are the same except for a simple change in scale, much as the early time data are similar to the later time data. If this were true, it would be possible to construct a scaling plot from both data sets such that all of the measurements fall on a single curve. This cannot be done with these two data sets because, while both have the same fractal exponent, they have different characteristic structure functions. The differing structure functions could be the result of qualitative differences in the behavior of the longer-range correlations in the two samples or, less likely, that the internal structure of the fractal aggregates comprising the gel differ in some way even though they have the same exponent.

Having measured the exponents in these gels from a scaling analysis, it is interesting to compare this to the result one would have obtained if a simple power-law analysis was performed on the same data. In Figs. 4a and 4b are plotted the same scaled data shown in Figs. 3a and 3b but this time with logarithmic axes. At higher wavevectors these plots show an approximately linear region from which a power-law exponent can be obtained. Instead

of reporting these slopes here, we have placed a triangle on each plot with a slope equal to that obtained by the scaling analysis. While the fit to the 30% sample is not as good as that to the 15% sample, it is clear that both methods give essentially the same value for the exponent.

This result, however, will in general not be true for all systems. There are two reasons for this: The first has been discussed above – both the correlations between the aggregates and the internal structure of the aggregates contribute to the diffraction effects and it is difficult to know their relative contributions. Apparently, in the two systems presented here the internal structure contribution dominates the scattering such that there is a region in which a power-law analysis is relatively weakly affected by correlations and thus yields a correct result. But this could not be assumed at the outset because there was no way of knowing to what extent the correlations contributed. The second reason is that the two methods actually measure two different properties of the system. That is, the scaling analysis provides a parameter defining how the system coarsens with time, whereas the power-law analysis measures a static structural property of the system. Fractal aggregation models predict that these two exponents will be the same but again this is not true in all models. For an example of an instance where the two methods yield completely different results see Ref. [7].

Acknowledgement

The SANS data were taken on the 30 m spectrometer supported by the National Science Foundation under Agreement No. DMR-9423101.

5. REFERENCES

[1] D. W. Schaefer, J.E. Martin, P. Wiltzius, and D.S. Cannell, *Phys. Rev. Lett.* **52**: 2371 (1984).

[2] G. Dietler, C. Aubert, D.S. Cannell, and P. Wiltzius, *Phys. Rev. Lett.* **57**: 3117 (1986).

[3] J.E. Martin and A.J. Hurd, *J. Appl. Cryst.* **20:** 61 (1987).

[4] R. Vacher, T. Woignier, J. Pelous, and E. Courtens, *Phys. Rev.* **B37**: 6500 (1988).

[5] M. Carpineti and M. Giglio, *Phys. Rev. Lett.* **68**: 3327 (1992).

[6] B.D. Butler, H.J.M. Hanley, D. Hansen, and D.J. Evans, *Phys. Rev. Lett.* **44**: 4468 (1995).

[7] B.D. Butler, D. Hansen, D.J. Evans, and H.J.M. Hanley, *Phys. Rev.* **B53:** 2450 (1996).

[8] B. D. Butler, C.D. Muzny, and H.J.M. Hanley, *J. Phys. Condens. Matter* **8**: 9457 (1996).

[9] The name Ludox SM-30 is used to identify the product. Endorsement by NIST is not implied.

[10] The condition for gelation is often tested by determining whether the sample keeps its shape when its container is tipped. This criterion is satisfied no later than 1 h after initiation for all of the samples studied here — well before the time that the scattering cross section becomes time invariant.

[11] B. D. Butler, H.J.M. Hanley, C.D. Muzny, and G.C. Straty, *Mat. Res. Soc. Symp. Proc.* **376**: 323 (1995).

[12] See for example, J. Marro, J.L. Lebowitz, and M.H. Kalos, *Phys. Rev. Lett.* **43**, 282 (1979); H. Furukawa, *J. Appl. Cryst.* **21**, 805 (1988).

[13] K. Schätzel and B.J. Ackerson, *Phys. Rev. Lett.* **68**, 337 (1992).

Figure Captions:

Figure 1: Measured neutron scattering cross sections as a function of time since gelation initiation for (a) 30% by mass and (b) 15% by mass colloidal silica samples.

Figure 2: Measured neutron scattering cross sections as a function of initial solution pH for gels made from (a) 30%, (b) 25%, (c) 20% , and (d) 15% by mass colloidal silica solutions. Measurements were made after the gelation reaction had completed.

Figure 3: The measured neutron scattering cross sections presented in Fig. 1 but scaled according to the relation give in the text.

Figure 4: Same scaled data as in Fig. 3 but plotted on logarithmic axes so that a power law slope might be extracted.

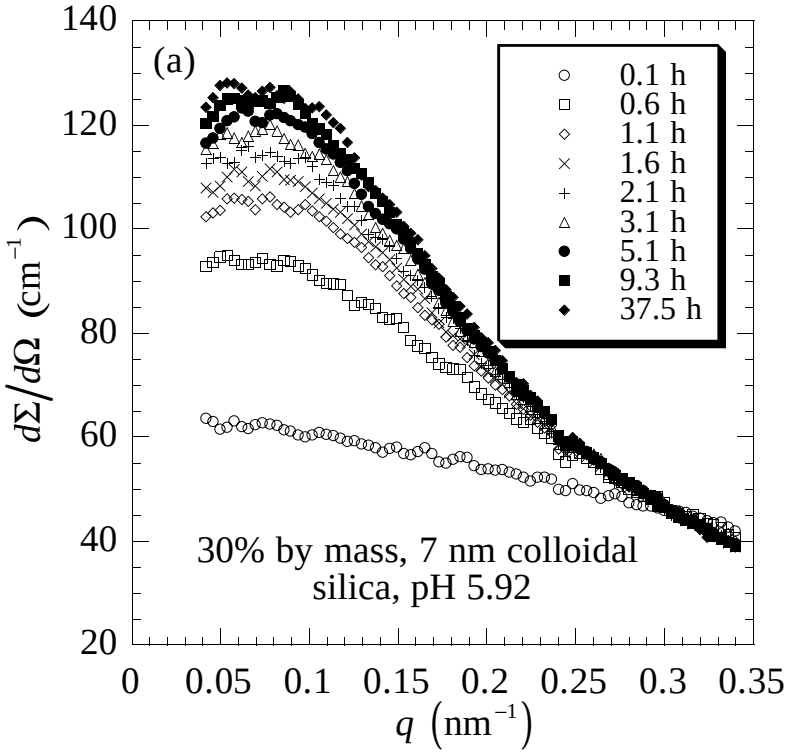
(a)
0.1 h
0.6 h
1.1 h
1.6 h
2.1 h
3.1 h
5.1 h
9.3 h
37.5 h
30% by mass, 7 nm colloidal silica, pH 5.92
dΣ/dΩ (cm⁻¹)
q (nm⁻¹)
140
120
100
80
60
40
20
0
0.05
0.1
0.15
0.2
0.25
0.3
0.35

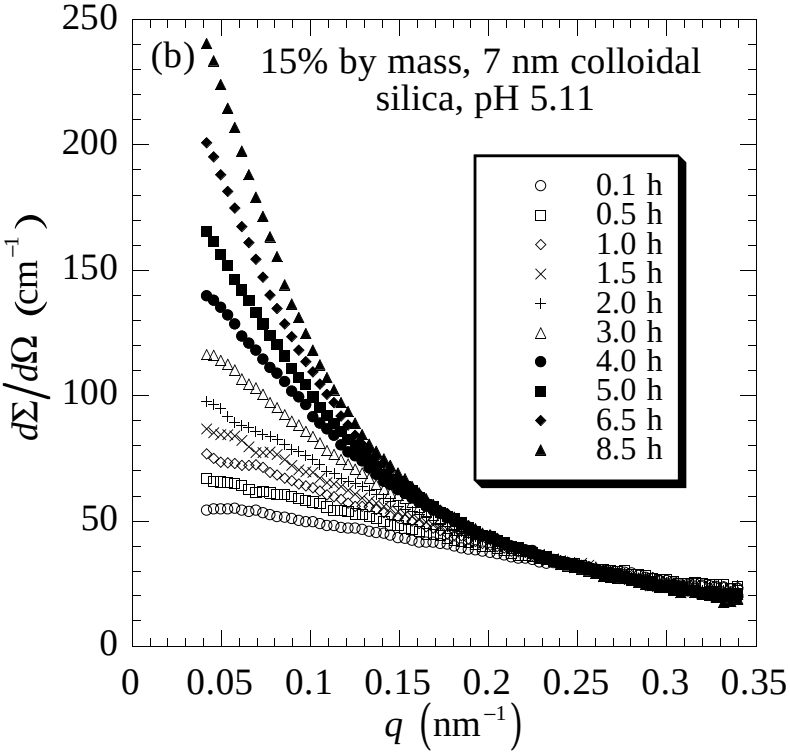
(b)
15% by mass, 7 nm colloidal silica, pH 5.11
0.1 h
0.5 h
1.0 h
1.5 h
2.0 h
3.0 h
4.0 h
5.0 h
6.5 h
8.5 h
dΣ/dΩ (cm⁻¹)
q (nm⁻¹)
250
200
150
100
50
0
0.05
0.1
0.15
0.2
0.25
0.3
0.35

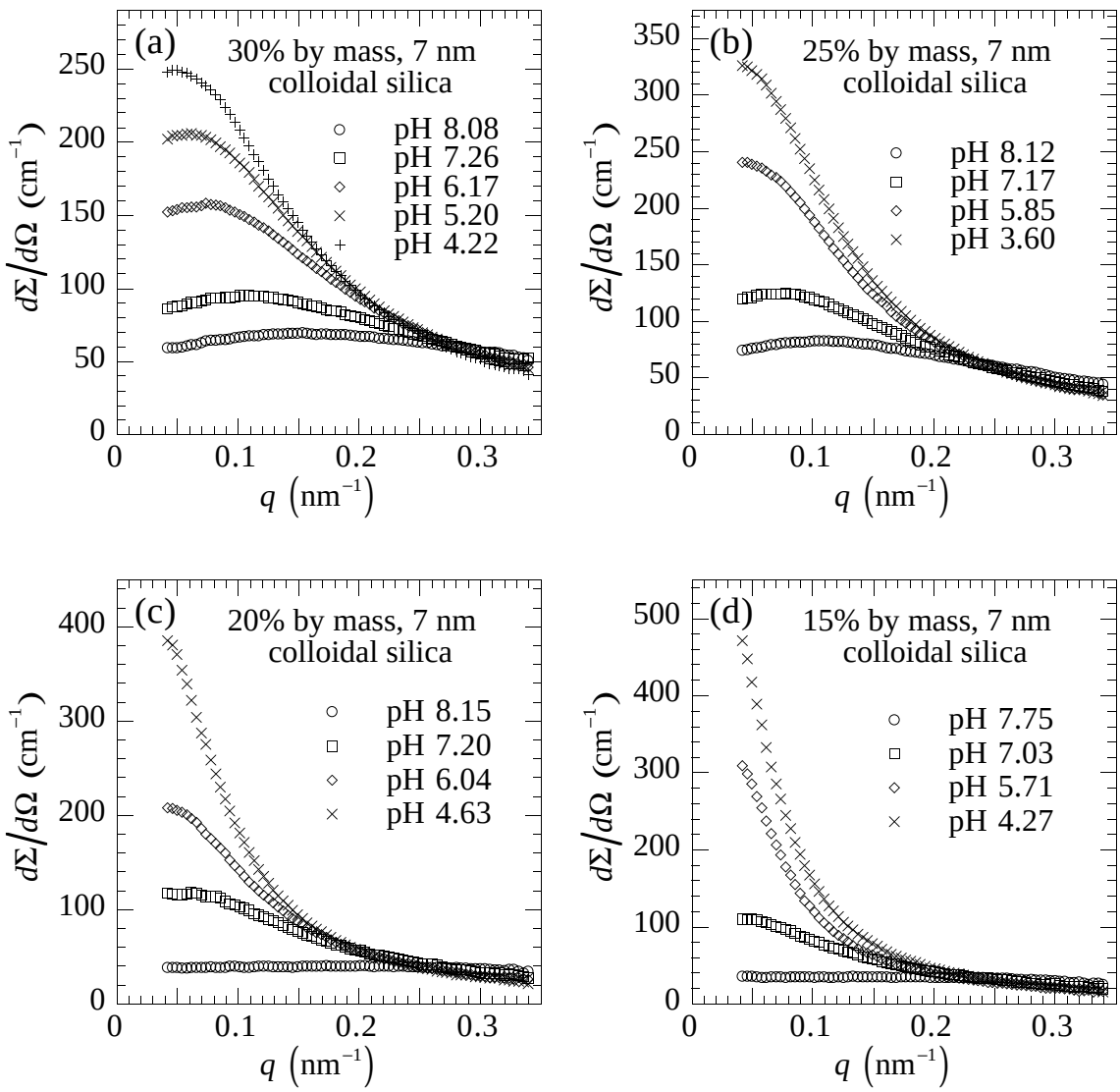
(a)
30% by mass, 7 nm
colloidal silica
pH 8.08
pH 7.26
pH 6.17
pH 5.20
pH 4.22
(b)
25% by mass, 7 nm
colloidal silica
pH 8.12
pH 7.17
pH 5.85
pH 3.60
(c)
20% by mass, 7 nm
colloidal silica
pH 8.15
pH 7.20
pH 6.04
pH 4.63
(d)
15% by mass, 7 nm
colloidal silica
pH 7.75
pH 7.03
pH 5.71
pH 4.27
dΣ/dΩ (cm⁻¹)
q (nm⁻¹)

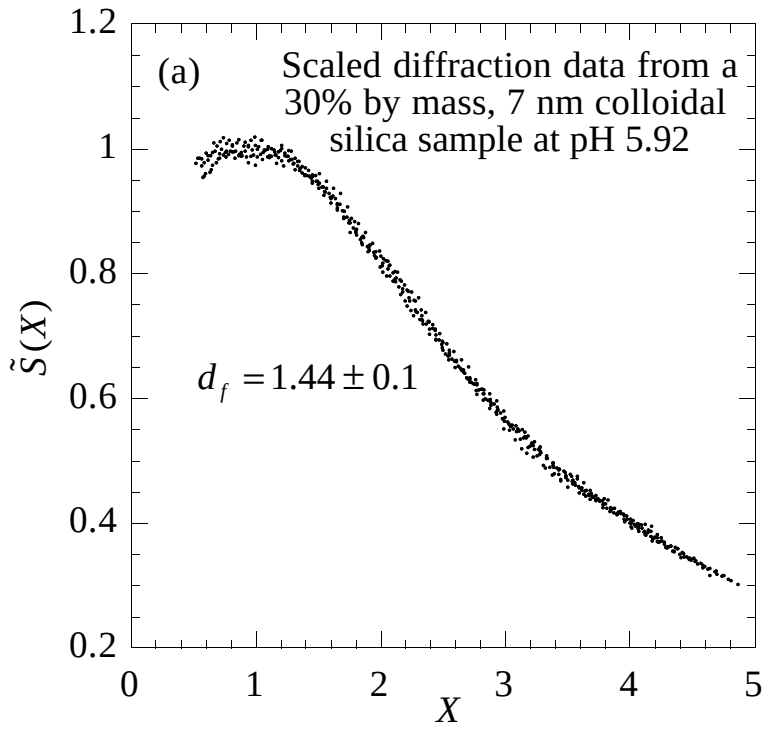
(a)
Scaled diffraction data from a 30% by mass, 7 nm colloidal silica sample at pH 5.92
$d_f = 1.44 \pm 0.1$
$\tilde{S}(X)$
X
1.2
1
0.8
0.6
0.4
0.2
0
1
2
3
4
5

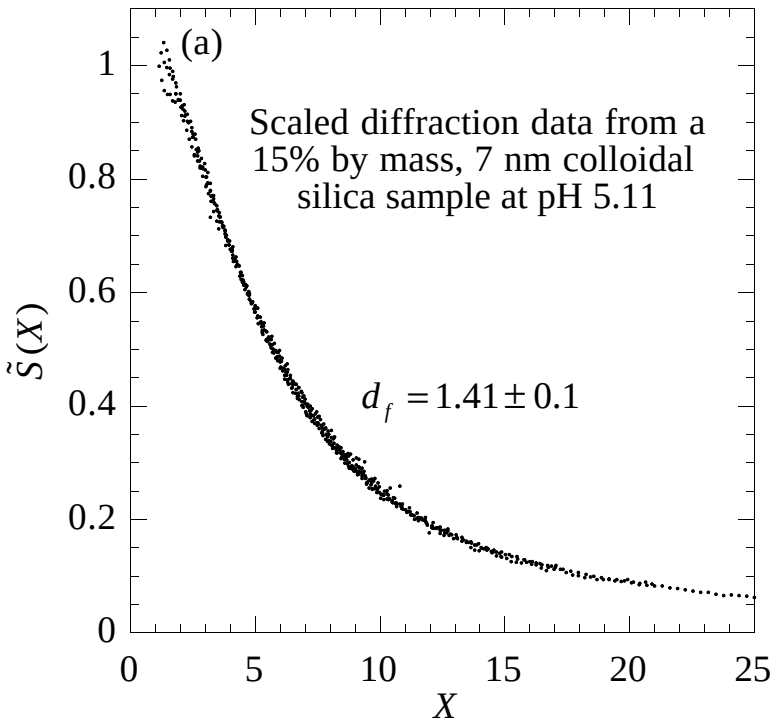
(a)
Scaled diffraction data from a 15% by mass, 7 nm colloidal silica sample at pH 5.11
$d_f = 1.41 \pm 0.1$
$\tilde{S}(X)$
X
1
0.8
0.6
0.4
0.2
0
5
10
15
20
25

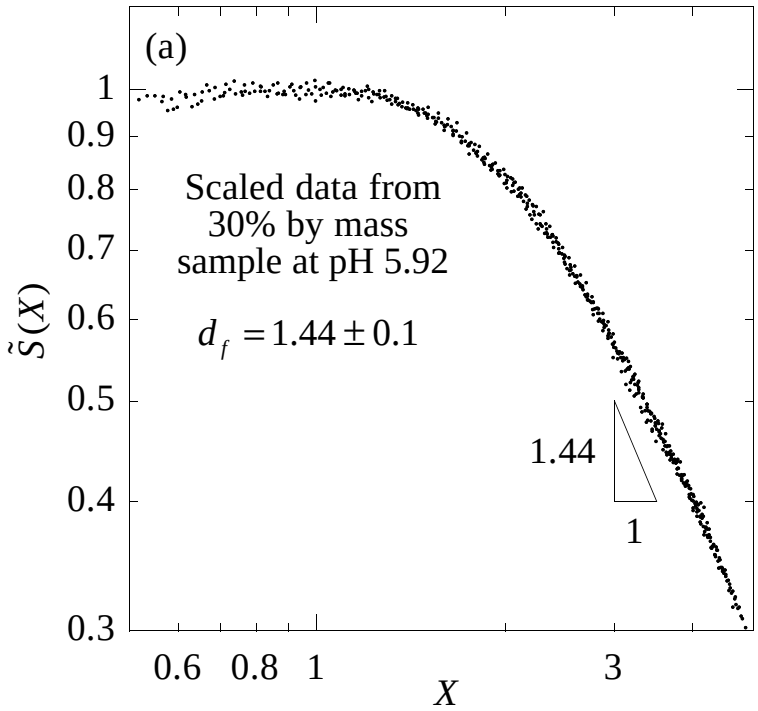
(a)
Scaled data from
30% by mass
sample at pH 5.92
$d_f = 1.44 \pm 0.1$
1.44
1
$\tilde{S}(X)$
1
0.9
0.8
0.7
0.6
0.5
0.4
0.3
0.6
0.8
1
3
X

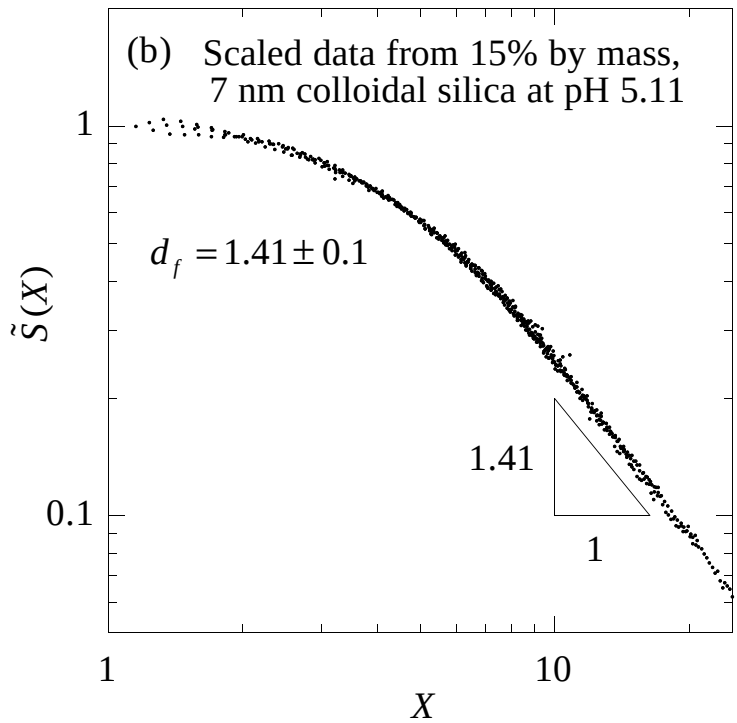
(b) Scaled data from 15% by mass,
7 nm colloidal silica at pH 5.11
$d_f = 1.41 \pm 0.1$
1.41
1
$\tilde{S}(X)$
1
0.1
1
10
X